The isoprenoid derivative N6-benzyladenosine (CM223) exerts antitumor effect in glioma patient-derived primary cells through the mevalonate pathway.

Elena Ciaglia,[a] Manuela Grimaldi,[b] Mario Abate,[a] Mario Scrima,[b] Manuela Rodriquez,[b] Chiara Laezza,[c] Roberta Ranieri,[a] Simona Pisanti,[a] Pierangela Ciuffreda,[d] Clementina Manera,[e] Patrizia Gazzerro,[b] Anna Maria D'Ursi*[b] and Maurizio Bifulco*[a,f].

[a]Department of Medicine, Surgery and Dentistry "Scuola Medica Salernitana", University of Salerno, Via Salvatore Allende, 84081 Baronissi Salerno, Italy

[b]Department of Pharmacy, University of Salerno, Via Giovanni Paolo II 132, 84084 Fisciano Salerno, Italy.

[c]Department of Biology and Cellular and Molecular Pathology, University of Naples Federico II, Via Pansini, 80131 Naples, Italy.

[d]Dipartimento di Scienze Biomediche e Cliniche "Luigi Sacco", Università degli Studi di Milano, Via G.B. Grassi 74, 20157 Milano, Italy.

[e]Department of Pharmacy, University of Pisa, Via Bonanno 6, 56126 Pisa, Italy.

[f]CORPOREA-Fondazione Idis-Città della Scienza, via Coroglio 104 e 57, 80124 Naples, Italy.

Funding: This study was supported by Associazione Italiana Ricerca sul Cancro (AIRC; IG 13312 and IG18999 to M. Bifulco). E. Ciaglia was supported by a fellowship from Fondazione Umberto Veronesi (FUV 2017, cod.1072).

Conflict-of-interest disclosure: The authors declare no competing financial interests.

Abstract:

Background and Purpose: N6-Isopentenyladenosine (i6A) is a modified nucleoside exerting in vitro and in vivo antiproliferative effects. We previously demonstrated that the i6A action is correlated to farnesyl pyrophosphate synthase (FPPS) expression and activity, a key enzyme involved in the mevalonate (MVA) pathway, which is found aberrant in brain cancer. To develop new anti-glioma strategies, we looked for other valuable compounds exhibiting improved activity as compared to i6A.

Experimental Approach: we designed and synthesized i6A derivatives characterized by the introduction of diverse chemical moieties in the N6 position of adenosine and tested for their efficacy in U87 and primary derived patient's glioma cell model. NMR based structural analysis, molecular docking calculations and siRNA mediated knock-down helped to clarify the molecular basis of their action, targeting FPPS protein.

Key results: We demonstrated that CM223, the i6A derivative including a benzyl moiety in N6 position of adenine, is endowed with a marked activity in selectively targeting glioma cells but not normal human astrocytes (NHA). This is achieved by the induction of intrinsic pathways of apoptosis and inhibition of proliferation along a FPPS-dependent protein prenylation blocking, which counteract the oncogenic signaling mediated by the epidermal growth factor receptor (EGFR).

Conclusion and Implications: This biological effect together with structural data on interaction of CM223 with FPPS, gain additional evidence on the correlation of the i6A/CM223 antitumoral activity with FPPS modulation. Because the MVA pathway is becoming an important promising target, CM223 and derivatives should be considered interesting active molecules in antiglioma pharmacological research.

Introduction.

N6-Isopentenyladenosine (i6A) is a modified nucleoside, formed by an adenosine harboring an isopentenyl chain derived from dimethylallyl pyrophosphate in the N6 position. It belongs to the cytokinin family, involved in control of many processes in plants. (Bifulco, Malfitano, Proto, Santoro, Caruso & Laezza, 2008; Kersten, 1984; Laten & Zahareasdoktor, 1985) In humans, many biological actions, both *in vitro* and *in vivo*, including antitumoral effects, can be attributed to i6A. (Castiglioni, Casati, Ottria, Ciuffreda & Maier, 2013; Laezza et al., 2014; Laezza et al., 2015; Pisanti et al., 2014; Woo et al., 2010; Ciaglia et al., 2017)

Interest in the study of this compound has been reinforced by our previous experimental observations that i6A interferes with the growth of k-ras transformed thyroid cells (KiMol) xenograft tumors by inhibiting farnesyl pyrophosphate synthase (FPPS) expression and activity (Laezza et al., 2006). Moreover i6A, exhibited immunomodulatory properties as it selectively expands and directly targets human natural killer cells through FPPS modulation (Ciaglia et al., 2013).

FPPS is a key enzyme involved in the mevalonate pathway and in downstream proteins prenylation; it catalyzes the two steps synthesis of the C15 isoprenoid farnesyl pyrophosphate (FPP), a crucial precursor for the synthesis of several classes of essential metabolites, such as sterols, ubiquinones and carotenoids. Therefore, FPPS plays a critical role in many vital cell reactions such as protein prenylation, synthesis of cell membrane constituents and signal transduction components. (Sacchettini & Poulter, 1997; Szkopinska & Plochocka, 2005) FPPS is currently the main biochemical target of bisphosphonates for the treatment of bone-related disorders, such as osteoporosis diseases, and metastatic bone-related tumors. However, as it is implicated in many cancer related pathways, and appears deregulated in many tumors, (Thurnher, Nussbaumer & Gruenbacher, 2012) it draws the interest of the pharmaceutical field in view of the identification of new specific anticancer compounds. (Fournier, Dauhine, Lundy, Rogers, Ebetino & Clezardin, 2008; Jahnke et al., 2010) Looking for molecular targets of i6A, using *in silico* inverse

virtual screening, (Chen & Zhi, 2001; Lauro, Romano, Riccio & Bifulco, 2011; Wang, Chu, Chen & Lin, 2012) we recently gained additional proofs that FPPS is a valuable molecular target for i6A.(Scrima et al., 2014) Saturation transfer difference (STD) NMR experiments and enzymatic assay indicated that i6A is able to bind FPPS active site exerting a moderate inhibition of its enzymatic activity (vide intra). (Ciaglia et al., 2013; Laezza et al., 2006) Indeed, molecular docking calculations evidenced that i6A is able to occupy the FPPS active site, with a significant contribution of the isopentenyl portion of the molecule. (Scrima et al., 2014)

Inspired by these data, in the search of a compound exhibiting improved activity as compared to i6A, we designed and synthesized i6A derivatives characterized by the introduction of new substituents in the N6 position of adenosine. (Scheme 1; See Supporting Information): insertion of a phenyl ring characterized by increasing steric hindrance at 6 position of adenosine (**FP11**, **FP13** and **FP16**), insertion, in the same position, of a benzyl ring (**CM223**) and double bond elimination (**CM224**). (Figure 1A). (Ottria, Casati, Baldoli, Maier & Ciuffreda, 2010)

All the compounds were tested for their anti-proliferative activity on U87MG and patients-derived primary glioma cells. Glioblastoma (GBM) is the most common and highly malignant brain tumor: recent work highlighted the importance of isoprenoid pathway, regulated by FPPS enzyme, for glioma development, progression and chemoresistance. (Laezza et al., 2015; Woo et al., 2010). Very recently it has been highlighted that GBM cells rely on cholesterol uptake for survival. (Villa et al., 2016) This provides new insights into more effective therapeutic strategies in GBM treatment, suggesting the repositioning of old class of drugs or the synthesis of new ones that modulates de novo cholesterol biosynthesis.

In this work we demonstrate that CM223, the i6A derivative including a benzyl moiety in N6 position of adenine, is endowed with a marked cytostatic and cytotoxic activity, higher than the parent compound i6A. NMR based structural analysis and molecular docking calculations, evidencing a clear structural interaction of CM223 with FPPS, further delineate the molecular basis to understand the interaction between i6A analogues and FPPS enzyme and the key events of

antiglioma action of these compounds. In this context the documented antiglioma action of CM223 was mediated primarily by the FPPS-dependent disruption of those lipid moieties which seem to be critical for the functionality and activity of epidermal growth factor receptor (EGFR) (Warren & Landgraf, 2006) and its downstream signaling proteins in glioma tumor growth and maintenance. (Furnari, Cloughesy, Cavenee & Mischel, 2015)

- **RESULTS**

Chemistry. **CM223** and **CM224** were prepared and purified as described previously. (Ottria, Casati, Baldoli, Maier & Ciuffreda, 2010) **FP11**, **FP13** and **FP16** were prepared modifying the synthetic route previously reported (Scheme S1; See Supporting Information). (Hocek, Holy, Votruba & Dvorakova, 2000) Purity of all compounds (≥ 99%) was verified by HPLC, nuclear magnetic resonance and mass spectrometry measurements. Structures of the aforementioned chemicals are presented in Figure 1.

Compounds **FP11**, **FP13** and **FP16** were obtained by the synthetic route described in the Scheme S1 (See Supporting Information).

BIOLOGICAL ASSAYS

Dose - response studies of the effects of i6A and its analogs on DNA synthesis of U87 glioma cells. The nucleoside i6A and its analogs **CM223**, **CM224**, **FP11**, **FP13**, **FP16** (whose chemical structures are shown in Figure 1A) were tested to compare their capability to inhibit the growth of U87MG human glioma cells. To this end U87 were incubated with increasing concentrations of the indicated compounds. In particular, as i6A had previously shown inhibitory activity in the range 0.3-20 μM, its analogs were tested for antiproliferative activity in the same range for 48h. As reported in Figure 1B, i6A-exposed glioma cells showed a dose-dependent inhibition of proliferation compared with untreated cells, as demonstrated by the BrdU incorporation assay. Interestingly the compound **CM223** elicited a more pronounced effect as compared to i6A (P≤

0.05) in the same conditions, whereas **CM224**, **FP11**, **FP13** and **FP16** compounds showed a lack of activity.

Analysis of the cytostatic and cytotoxic potential for the i6A derivative CM223 on U87 glioma cells and normal primary astrocytes. The growth inhibitory effect of **CM223** was further investigated at different time points by proliferation and clonogenic assay. i6A – whose anti - glioma effect has recently reported by our group (Ciaglia et al., 2017) was used as reference. Specifically the anti-proliferative capacity of increasing concentrations of i6A or **CM223** in a 0.3-20 μM concentration range was assessed in time course (24-72 h) on proliferating U87MG cells by BrdU incorporation assay (Figure 2A). After 48 h treatment, i6A-exposed glioma cells showed a dose-dependent inhibition of proliferation compared to untreated cells; in particular, a clear reduction of proliferative rate became evident at a concentration of about 7.5 μM. Of note, **CM223** elicited a more significant reduction of U87MG proliferation as compared to i6A-treated cancer cells, as a significant response was already achieved at a concentration of 1.2 μM. Of course, this inhibitory effect on proliferating cells became more evident after 72 h - treatment. Interestingly, **CM223** was able to exert a more significant effect also on the formation of clones (Figure 2B). Indeed a reduction of number and dimension of clones was registered already in cells treated with the lowest concentrations of **CM223** 1 μM and 2.5 μM.

To assess whether the inhibition of cell proliferation by i6A and especially by **CM223** was also associated to the induction of apoptosis, we performed a cytofluorimetric cell death analysis by Annexin-V and propidium iodide staining. i6A and **CM223** exhibited a dose-dependent activity to induce apoptosis when glioma cells were treated for 48 h (Figure 2C, *upper panel*). Interestingly even in this experiment, the percentage of cells in early and late apoptosis after **CM223** treatment was significantly higher as compared to i6A treatment, overall suggesting a better cytostatic and cytotoxic potential for this i6A derivative. Interestingly **CM223** elicited no significant reduction of

normal human astrocyte (NHA) cell viability as compared to cancer cells in the same condition (Figure 2C, *lower panel*).

FPPS-CM223 structural interaction: NMR spectroscopy

We have previously demonstrated that i6A interferes with the growth of k-ras transformed thyroid cells (KiMol) xenograft tumors by inhibiting FPPS expression and activity (Laezza et al., 2006); moreover the immunomodulatory activity of i6A is proved to occur through FPPS modulation (Ciaglia et al., 2013). Preliminary NMR data and colorimetric enzymatic assay evidenced that i6A interacts with FPPS binding site inducing a moderate inhibition of its activity.

Following the screening for the cytostatic and cytotoxic activity of i6A analogs (Figure 1) and to confirm that activity of these compounds occurs even through FPPS inhibition, we analyzed by STD NMR experiments (Mayer & Meyer, 1999; Mayer & Meyer, 2001) i6A analogues reported in Figure 1 for their ability to interact with FPPS protein. (Figure 3A). STD is a powerful NMR technique that enables the identification of new protein-ligands enabling the determinations of protein-ligand dissociation constants (K_D). NMR sample containing 8.0 μM of FPPS was titrated with i6A-analogs to have STD build-up at protein-ligand molar ratios: 1:10, 1:20, 1:30, 1:50, 1:70, and 1:100. For each titration point, STD experiments were carried out using different saturation times (0.50, 1.00, 1.50, 2.00, 3.00, 4.00, and 5.00 s).(Angulo & Nieto, 2011) Standard ^{1}H monodimensional and 2D COSY NMR experiments allowed the 1H chemical shift assignment of i6A-analogs proton signals. (Figure S2-S6; See Supporting Information)

Analysis of STD-NMR experiments for the compounds **CM223** and **CM224** characterized by the insertion of the benzyl (**CM223)** and isopentyl moiety (**CM224)** indicates a marked interaction with the enzyme, with an important participation of the adenosine moiety (in particular protons H2-H8, H4”-H8”, H5”-H7”, H6” and H1’). These effects reached the significant value of 30% **CM223** and 20% **CM224** respectively. (Figure 3A) The compounds of FP series, containing the aromatic ring directly linked to the 6-position of adenosine, show less marked interactions. (Supplementary

material, Figure S1) To confirm that i6A analogues (Figure 1A) bind FPPS active site instead of allosteric binding site, (Jahnke et al., 2010) FPPS-ligand complexes were titrated with increasing concentrations of *3-carboxymethyl-5,7-dichloro-1H-indole-2-carboxylic acid* (allosteric modulator IC_{50} = 6.0 μM) (Jahnke et al., 2010) and zoledronic acid, high affinity FPPS inhibitor (data not shown). (Scrima et al., 2014) The quantitative evaluation of STD data confirm that the compound **CM223** interacts with FPPS binding site with a consistent contribution of the N6 substituents.

We calculated the K_D for the complex FPPS-**CM223** interaction based on the quantitative measurement of STD effects (Figure 3B). We collected experiments at different protein-ligand ratios and saturation time conditions, according to the methodology developed by Angulo et al. (Angulo & Nieto, 2011). Using this procedure, the calculation of protein-ligand affinities is independent from contingent experimental factors, such as STD saturation time, ligand residence time in the complex, and the intensity of the signal. (Angulo & Nieto, 2011)

NMR sample containing 8 μM of FPPS was titrated with **CM223** to have STD build-up at protein-ligand molar ratios: 1:10, 1:20, 1:30, 1:50, 1:70, and 1:100. For each titration point, we recorded STD experiments using different saturation times (0.50, 1.00, 1.50, 2.00, 3.00, 4.00, and 5.00s). The mean K_D value calculated for the single protons of **CM223** (Figure 3B) is 0.19 mM. This value, that is 5 fold lower as i6A-FPPS K_D value, (Scrima et al., 2014) indicates an improvement in the binding with FPPS target for **CM223** and suggests that the newly introduced benzyl portion of the molecule may lead to more active FPPS inhibitors.

Interprotonic distances calculated on the basis of STD NMR experiments were imposed as restraints in molecular docking calculations (AutoDock 4.2 software) (Morris et al., 2009). Compounds **CM223** and **FP13,** respectively representative of the most and least FPPS binders, were subjected to molecular docking simulations against 3D FPPS protein model (PDB code: 1ZW5), selected in inverse virtual screening procedure in our previous work (Scrima et al., 2014; Kavanagh et al., 2006) For an exhaustive exploration of conformational space, iterative docking calculations consisting of 250 runs were executed, yielding 1500 structures. The resulting binding

poses were clustered together according to positional rmsd (rmsd< 3.5 Å). Docking analysis revealed a favorable accommodation of i6A analogues in the binding site of FPPS through a large set of both hydrophobic and polar interactions (Figure 3D). Sugar moiety establishes a network of H-bonds with Asp118, Asp257 and Lys271.

Adenine core of the molecule is oriented between the three Mg ions co-crystallized with FPPS, making polar contacts with Lys214, Asp257 and H-bonding with Gln254. In CM223, the benzyl portion, analogously to isopentenyl moiety of i6A, is placed in the deeper region of the binding site and engages pi-stacking interactions with Phe113, and Tyr218 of the enzyme. (Scrima et al., 2014) The increased binding of **CM223** (Kd 0.19 mM) as compared to i6A (Kd 1.0 mM) may be due to these interactions that in **CM223** are stabilized by the presence of the aromatic benzyl ring instead of the isopentenyl chain. Concerning **FP13**, the difference in the binding mode as compared to i6A and CM223 is due to the phenyl ring that represents a low flexibility point for this molecule. STD NMR data, on the contrary show that the weak binding of FP13 with FPPS catalytic pocket is based on interaction of ribose sugar moiety.

FPPS colorimetric assay. To test whether the interaction of **CM223** with FPPS, observed in NMR data, might result in an enhancement of enzyme inhibition compared to i6A, we performed a colorimetric assay. (Gao et al., 2010)

The histograms in Figure 3C show FPPS activity after the pre-treatment with **CM223** (from 0.1 to 5 mM, 30 min 37 °C) or i6A (from 1.0 to 5 mM, 30 min 37 °C) used for comparison. Enzymatic activities of FPPS in absence and in presence of high affinity FPPS inhibitor, zoledronic acid (1-2 µM, 30 min 37 °C) are reported as negative and positive controls. As expected, even though far away from the inhibition efficiency achieved by the bisphosphonate, the curves indicate a trend of inhibition of FPPS activity by i6A and to a more extent by **CM223,** with an EC50 value of 5.33 mM and 3.33 mM respectively. This suggest that the modulation of enzyme activity by **CM223** is

really improved with respect to the isoprenoid counterpart i6A, even if we cannot rule out the targeting of other enzymes of the pathway beyond the FPPS.

CM223 acts on U87 glioma cells via FPPS modulation and disruption of lipid dependent-EGF receptor signaling pathway.

In order to verify that **CM223** anti-proliferative and pro- apoptotic effects on U87 glioma cells were associated with its capacity to interfere with the mevalonate pathway in terms of FPPS modulation, first we moved to test the ability of CM223 to inhibit post-translational modification of small GTP-binding proteins, by analyzing the prenylation status of Ras-proximate-1 or Ras-related protein 1 (Rap1A). Rap1A is a protein prenylated exclusively by GGTase, and its unprenylated form is recognized by a specific unprenylated anti-Rap1A antibody. U87MG cells were treated with i6A, **CM223** and Zoledronic acid (ZA) for comparison, for 24 h. In control epidermal growth factor (EGF)-treated U87 cells, Rap1A was in the processed prenylated forms, so not detected in western blot analysis. As expected, by acting through FPPS modulation, treatment with ZA or i6A and to a more extent with **CM223** inhibited the processing of Rap1A, resulting in increased level of unprenylated Rap1A form (Figure 4A). Interestingly the transfection of U87MG cells with FPPS siRNA increased their sensitivity to CM223. Indeed, while FPPS siRNA transfection alone did not modify the unprenylated Rap1A expression kinetic, probably due to a residual activity of the enzyme after its knock-down which guarantee the sufficient synthesis of isoprenoid (or other lipid) moiety, (Wang, Panasiuk & Grainger, 2011) in FPPS siRNA-CM223 co-treatment, the induction of unprenylated Rap1A expression by CM223 was more evident (Figure 4B), suggesting a more complete inhibition of FPPS activity achieved by the combination. At the same way a parallel accumulation of Ras in its unprenylated form, seen as an “up-smearing” on immunoblots, has been also highlighted. Overall these data point out to FPPS as a possible target of action of CM223. As lipid environment of plasma membranes and lipids-proteins interaction have been proposed as molecular platform important for oncogenic signaling processes, (Warren & Landgraf, 2006) then

we moved to test the influence of CM223 on the activity of receptors embedded in the membrane. Among them, the epidermal growth factor receptor (EGFR, also referred to as ERBB1 or HER1), is a well-known oncoprotein belonging to HER superfamily of receptor tyrosine kinases together with ERBB2, ERBB3, and ERBB4. It constitutes the most common genetic alteration associated with malignant glioma where its over-activation and/or overexpression is responsible for the deregulation of pleiotropic cellular processes, including cell differentiation, metabolism, proliferation, and survival. (Furnari, Cloughesy, Cavenee & Mischel, 2015) As expected the stimulation with EGF induced an early activation of EGF receptor (10 min) by significantly increasing the EGFR phosphorylation on tyrosine 1068 (Figure 4C). As consequence the rapid activation of downstream Signal transducer and activator of transcription 3 (STAT3) signaling pathway was achieved. In this experimental setting the importance of lipid environment in EGFR physiology was highlighted by the treatment with the membrane impermeable, small cyclic oligosaccharide methyl-β-cyclodextrin (MβCD). Indeed through the disorganization of lipid rafts by mean of cholesterol extraction, MβCD was able to alter receptor signaling by reducing the downstream phosphorylation levels of STAT3 in response to EGF (Figure 4C, *left panel*). The recovering from cholesterol depletion and the inhibition by MβCD was totally reversed after 3h from its removal even in the absence of added serum, mainly due to lipid synthesis in the cells. As consequence Simvastatin, an inhibitor of cholesterol synthesis, but to a much extent CM223 did inhibit the recovery of EGF-induced STAT3 signaling (Figure 4C, *right panel*), strengthening the hypothesis that the i6A analogue CM223 significantly interfere with the mevalonate metabolic pathway.

CM223 selectively inhibits the oncogenic AKT and STAT3 signaling and induces apoptosis, activating intrinsic caspase cascade in cultured U87 glioma cells.

It is well characterized that Protein kinase B (PKB)/AKT, STAT and Ras-MAPK (ERK) pathways, which regulate cellular growth, proliferation, and survival, are downstream players of

EGF receptor tyrosine kinase. (Hackel, Zwick, Prenzel & Ullrich, 1999) Then to investigate if EGFR signaling interference by CM223 significantly affect this downstream cellular pathway, we treated U87 cells for 24 h with effective increasing concentrations of the nucleoside prior to assay proteins for western blot analysis. We found that, at all doses tested, **CM223** significantly suppressed AKT and STAT3 activation in cultured U87 glioma cells, reflected by the reduction of the phosphorylation levels of AKT (Ser 473) and of STAT3 (Tyr 705) (Figure 5A). As regard as MAPK/ERK pathway, its inhibition, in term of reduction of phosphorylation of activation loop residues Thr202/Tyr204, is achieved only for the concentration of **CM223** ranging from 1 to 5 µM. On the contrary in response to 10 µM **CM223** treatment, we documented a sustained ERK phosphorylation. In this context several reports (Wei, Yan & Tang, 2011) suggested that ERK activation can also play an active role in mediating apoptosis, functioning upstream of caspase activation to initiate the apoptotic signal. In T98G cells activation of ERK was observed in response to cisplatin and UV light and was shown to strongly promote apoptosis in these GBM cell line. (Hamdi et al., 2008) To verify this hypothesis and to corroborate the proapoptotic effect of **CM223**, we examined the expression of caspases and key proteins that play essential roles in apoptosis induction. Treatment of 24h with CM223 strongly induced the expression of cleaved caspase-9, cleaved caspase-7 and -3, as well as cleaved PARP, in a concentration-dependent manner (Figure 5B), without affecting caspase 8 activity, which suggests the **CM223** induced execution of the apoptotic cell intrinsic program. The expression of proapoptotic Bim and antiapoptotic Bcl-2 and Bcl-XL proteins was further examined to explore the mechanism of **CM223**-induced apoptosis. The decreased expression of Bcl-XL, canonical transcriptional target of AKT, well fits with its inhibition by **CM223**, as well as the marked increase in the levels of the three major Bim isoforms (Bim EL, L, S) well correlates with the presence of the cleaved form of PARP and with the inactivation of AKT and of Bim negative regulator ERK. In keeping with these observations, phosphorylation of ERK was down-regulated by **CM223** treatment which lead to a concomitant induction of the levels of the pro-apoptotic Bim and to a clear caspase 3 cleavage induction (Figure

5B). Interestingly, in control normal compartment, we were hardly able to detect Bim and caspase 3 cleavage induction as compared to cancer cells in the same condition (Figure 5C). These results corroborate the inability of CM223 to affect NHA cell viability (Figure 2C) suggesting its specificity of action for tumor compartment with minimal cytotoxic effects on normal brain.

Analysis of sensitivity of primary glioma patient-derived cells to CM223 treatment.

To test its efficacy in a more physiopathological context *ex vivo*, we moved to characterize the sensitivity of two representative glioma patients-derived cell lines (GBM37 and GBM50) to CM223 treatment. As shown, CM223 (10µM) inhibited the phosphorylation of STAT3 in all glioma cells either when the signaling operated constitutively either when EGFR was activated by EGF stimulus (50 ng/ml) which, as expected, results in the physiological degradation of the receptor in order to protect the cell from overstimulation (Figure 6A and Figure 4C) (Sigismund et al. 2013). Interestingly, the degree of inhibition was more pronounced in primary cells compared to U87 glioma cell line. Accordingly in GBM cells CM223 achieved a 50% growth inhibition (IC50) at lower concentrations than in U87 cells (Figure 6B), that is 1,2 µM in GBM37 primary cell line and 0.45 µM in those derived from GBM50 tumor *versus* 1.9 µM in U87 (Figure 6B). Even though by different mechanisms, CM223 and (EGFR) tyrosine kinase inhibitor Erlotinib share the same target, so the empirical combinations of these drugs was finally tested in U87 and GBM cell lines. For Erlotinib the fixed concentration of 0.6 µM was chosen. Interestingly, CM223, was more active than Erlotinib in reducing proliferation of glioma cells in the same condition (-37% *vs* -20% in U87; -35% *vs* -10% in GBM37; -60% *vs* -40% in GBM50) which was additionally reduced by drug combination (-60.6% in U87; -58,8% in GBM37; -72% in GBM50).

Although the extrapolation of *in vitro* data to the clinical setting should be considered with caution, these last preliminary results may have implications for the rational development of new chemotherapeutic regimens, including Erlotinib and CM223 or derivatives for the treatment EGFR-driven cancers.

DISCUSSION

We have demonstrated that i6A exerts cytotoxic, antiangiogenic and proapoptotic activity in different cell lines. (Ciaglia et al., 2017; Laezza et al., 2009; Laezza, Malfitano, Di Matola, Ricchi & Bifulco, 2010; Laezza et al., 2006; Pisanti et al., 2014; Spinola, Colombo, Falvella & Dragani, 2007)

Previous reports by our group highlighted the involvement of FPPS in i6A action in different physiopathological settings. (Ciaglia et al., 2013; Laezza et al., 2006) More recently we documented for the first time the antitumor activity of i6A on human glioma cells. (Ciaglia et al., 2017) In our work, i6A clearly displayed antiglioma action through AMP-activated protein kinase (AMPK)-dependent internalization and degradation of EGFR; however, we have to take into account that it might also elicit other effects. Indeed, i6A reduces the growth of xenograft tumors induced by k-ras transformed thyroid cells (KiMol) by inhibiting farnesyl pyrophosphate synthase (FPPS), a key enzyme of the isoprenoid biosynthetic pathway and protein prenylation, (Laezza et al., 2006) which are crucial events for the function and activity of EGFR and its downstream signaling. Moreover using an inverse virtual screening approach and NMR spectroscopy experiments, we showed that i6A is able to bind FPPS active site determining a moderate enzyme inhibition. All these evidence, and in particular the study of the i6A binding in the FPPS site, inspired the design of new analogs carrying different substituents at the N6 position of the purine ring. As an important contribution of the isopentenyl moiety was demonstrated in the binding of i6Awith FPPS enzyme, we designed and synthesized the analogs shown in Figure 1A, including a benzyl ring (**CM223**) and an isopentyl moiety (**CM224**) or a diversely substituted phenyl ring (compounds **FP11**, **FP13** and **FP14**), (Ottria, Casati, Baldoli, Maier & Ciuffreda, 2010)

In view of advancing chemotherapeutic administration-targeted drug therapy for glioblastoma, that is the highest malignant SNC tumor, i6A analogs were studied in cell growth experiments on U87MG human glioma cells and patients primary derived cells: in these conditions, only **CM223** exhibited a marked cytostatic effect significantly higher as compared to that of i6A, whereas the

others showed an irrelevant activity. According to STD-NMR experiments and enzymatic colorimetric assay **CM223** cytostatic activity, analogously to i6A, was related to the modulation of FPPS. Interaction of **CM223** with FPPS active site was regulated by a KD 5 fold lower as i6A and an EC50 two fold lower than i6A. Interestingly, compounds **CM224** and **FP13** showing no significant cytostatic effect, exhibited no-significant STD effects, confirming the relationship between the antiproliferative activity and the FPPS binding. Interpretation of these data in the light of SAR considerations, corroborated by molecular modeling calculation, indicates that the increased binding of **CM223** (Kd 0.19 mM) as compared to i6A (Kd 1.0 mM) is due to the presence of the aromatic benzyl ring that engages more stable pi-stacking interactions with Phe113, and Tyr218 of the enzyme. Concerning FP13, the difference in the binding mode as compared to i6A and CM223, is due to the phenyl ring that represents a low flexibility point for to this molecule.

A more detailed investigation of the **CM223** antiproliferative action has evidenced an its marked anti-clonogenic effect, associated to higher pro-apoptotic action as compared to i6A. Exploration of the cellular pathway through which **CM223** elicited these effects evidenced the ability to suppress AKT and STAT3 activation, whose signaling is critical for glioma cell proliferation and survival. The effect of **CM223** on MAPK/ERK pathway was concentration dependent, as it appeared inhibitory at concentration ranging from 1 to 5 μM, but stimulatory at 10 μM. According to several reports (Hamdi et al., 2008; Wei, Yan & Tang, 2011), these results may be interpreted considering that ERK activation can also induce apoptosis upstream of caspase activation. Indeed **CM223** proved to be responsible of several molecular events coherent with the execution of the apoptotic cell intrinsic program: induction of cleaved caspase-9, cleaved caspase-7 and -3; induction of PARP cleavage, without effect on capase 8. Moreover, **CM223** increased the levels of the proapoptotic three major Bim isoforms (Bim EL, L, S) and decreased the expression of antiapoptotic Bcl-XL.

Looking for the putative molecular mechanism, we highlighted that anti-glioma action of CM223 is related to the modulation of mevalonate pathway and at least in part, to FPPS targeting. The observation of increased levels of unprenylated form of the small GTPase Rap1A in response to

CM223 (Figure 4B) and the more complete inhibition of FPPS activity achieved by the FPPS siRNA-CM223 combination (Figure 4C), along NMR interaction data might suggest a direct effect on FPPS enzyme. However a little discrepancy between the potency of the compound in NMR and FPPS colorimetric assays, where CM223-FPPS direct interaction was uniquely explored, and that exibited in a more complex cellular model was documented. Here, the higher efficiency of CM223 in inhibiting the cell growth of tumor cells through the cholesterol depletion (Fig. 4C) suggests that CM223 does really interfere with the MEV metabolic pathway; however the FPPS might not be the unique key target of its action and a bystander influence of other key enzymes and intermediate metabolites of mevalonate and isoprenoid pathway, modulated by CM223, cannot be ruled out. On the other hand the better efficiency of the compound in culture cells might be due to its conversion in a more active metabolite inside the cells, as previously documented for i6A that must be monophosphorylated into 5'-i6A-monophosphate by the adenosine kinase to exert its inhibitory effects on HUVEC endothelial cells. (Pisanti et al., 2014).

Anyway several reports in literature show the correlation between the FPPS inhibition and the cytostatic and/or pro-apoptotic effects. Of note it is demonstrated that overactive prenylated Rap1A, enhanced the proliferative capacity of certain cell types contributing to tumorigenesis. (Frische & Zwartkruis, 2010; Jeyaraj, Unger & Chotani, 2011) Moreover accumulation of unprenylated Rap1A due to the inhibition of farnesyl- or geranyl geranyl trasferase *in vitro*, induced apoptosis in human plasma cells suggesting that geranylgeranylated proteins, like Rap1A, play a role in signaling pathways that prevent cell death. (Gordon et al., 2002) Here we showed that the disruption of lipid moieties by CM223-mediated FPPS inhibition was critical for the functionality and activity of epidermal growth factor receptor (EGFR) (Warren & Landgraf, 2006) as potently impairs the main intracellular signaling pathways responsible for the mantainance of neoplastic phenotype. Prenylation is indeed required for the proper function and localization of several downstream critical mediators of the EGFR signaling cascade, including the Ras, Rho, and Rab families, which require farnesyl and geranylgeranyl post-translational modifications for their activity. (Gibbs, Oliff

& Kohl, 1994) Moreover it is well known that the isoprenoid compound dolichol is involved in the N-linked glycosylation of EGFR, which facilitates its proper conformation and efficient ligand binding and activation of EGFR. (Carlberg et al., 1996; Ceresa & Bahr, 2006) Accordingly we highlighted the inability of CM223-treated cells to properly re-establish the endogenous mevalonate and isoprenoid levels and recover EGFR signaling after washout of MβCD (Figure 4C). Consistent with these mechanism of action, we observed that CM223 is highly efficacious at blocking tumor cell growth of EGFR-activated primary GBM cells in which the EGF-induced signaling sensitizes them to CM223 effect. Last, by indirectly targeting EGFR, CM223 has been seen to ameliorate the response to EGFR-TKI Erlotinib when given in combination (Figure 6B).

In view of the results collected in our experiments and considering the evidence reported in literature, we may be confident that the antiproliferative and proapoptotic effects of **CM223** in glioma cells, may be in part ascribable to the EGFR signaling perturbation, as consequence of the modulation of metabolic pathway of the mevalonate and in particular of FPPS key branch point enzyme

Indeed, we demonstrated by STD-NMR experiments that **CM223** binds and inhibits FPPS activity. Interaction of **CM223** with FPPS active site was regulated by a K_D 5 fold lower as i6A and an EC50 two fold lower than i6A. Interestingly compounds **CM224** and **FP13** showing no significant cytostatic effect, failed to bind FPPS enzyme in STD-NMR experiment, confirming the relationship between the antiproliferative activity and the FPPS binding. Interpretation of these data in a SAR perspective, corroborated by molecular modeling calculation, indicates that the difference in the binding of **CM223** as compared to the compounds of FP series is due to the phenyl ring that infers rigidity to this molecule portion.

CONCLUSIONS

Taken together our data confirm that i6A and in a much extent its benzyl analog **CM223** are endowed with a promising antitumoral activity on glioblastoma cells. The modification we adopted

on i6A scaffold leads to molecules that can be considered lead compounds in antiglioma pharmacological research. Indeed the *in vitro* **CM223** efficacy, the lack of cytotoxicity on healthy brain cells, its additional activity in patients-derived primary GBM cells that more accurately reflect the physiopathological context, make **CM223** an interesting compound for the development of novel valid chemotherapeutic agents in glioma and other EGFR-driven cancers.

All the biological pathways (*vide intra*) controlled by i6A (Ciaglia et al., 2013; Laezza et al., 2006) and **CM223** are related to the inhibition of FPPS enzyme, therefore the development of i6A analogs characterized by increased antitumor activity may take advantage of the FPPS-**CM223** structural interaction data.

MATERIALS AND METHODS

General Procedures. Organic solvents were purchased from Sigma-Aldrich (St. Louis, MO, USA). and dried in the presence of appropriate drying agents and were stored over suitable molecular sieves. Melting points were determined on a Kofler® hot stage apparatus and are uncorrected. ^{1}H NMR spectra were recorded with a Bruker Avance-500® spectrometer in δ units with TMS as an internal standard. Mass spectra were performed with a Hewlett-Packard MS system 5988®. TLC was performed on silica gel sheets (Silica Gel 60 F254, Merck, Germany). Microwave-assisted reactions were run in a CEM microwave synthesizer. The system for isocratic flash chromatography includes a Buchi® Pump Module C-601 (continuous flow of solvents up to 250 ml/min at max 10 bar) and Buchi® prepacked cartridges (silica gel 60, particle size 40-63 μm). The purity was determined by high performance liquid chromatography (HPLC) Shimadzu system using analytic C18 Phenomenex column. Purity of all final compounds was 99%.

Reagents and Abs. N6-isopentenyladenosine (i6A), Zoledronic acid monohydrate (Sigma-Aldrich, St. Louis, MO, USA), methyl-β-cyclodextrin (MβCD), Simvastatin, a synthetic analog of lovastatin, and erlotinib were purchased from Sigma–Aldrich (St. Louis, MO, USA); Epidermal

growth factor (EGF) was diluted in a buffer containing a stabilizer (5% Trehalose) and added to cell cultures at the indicated concentration. Human EGF was purchased from Peprotech (London, UK). (St. Louis, MO, USA).

In transfection procedure Lipofectamine 3000 were from Invitrogen. Optimem were from Gibco (#51985). For western blot analysis the following antibodies were used: rabbit polyclonal anti-human β-actin, rabbit polyclonal anti-human ras and rabbit polyclonal anti-human FPPS were purchased from Abcam (Cambridge, UK), mouse monoclonal anti-human α-Tubulin from Sigma-Aldrich Inc. (St Luis, MO, USA), rabbit polyclonal anti-human cleaved Caspase-3, rabbit polyclonal anti-human Rap1A, rabbit polyclonal anti-human Caspase-3, rabbit monoclonal anti human cleaved caspase-9, rabbit monoclonal anti-human Caspase-9, rabbit monoclonal anti-human Caspase-7, rabbit monoclonal anti-human cleaved Caspase-7, rabbit monoclonal anti-human cleaved Caspase-8, rabbit monoclonal anti-human Bim, rabbit monoclonal anti-human Bcl-2, rabbit monoclonal anti-human Bcl-xL, rabbit polyclonal anti-human phospho-STAT3 (p-STAT3; Tyr705), rabbit monoclonal anti-human STAT3, rabbit monoclonal anti-human Cleaved PARP (Asp214), rabbit monoclonal anti-human PARP, rabbit monoclonal anti-human Phospho-p44/42 MAPK (p-Erk1/2; Thr202/Tyr204), rabbit monoclonal anti-human p44/42 MAPK (Erk1/2), rabbit monoclonal anti-human Phospho-Akt (p-Akt; Ser473), rabbit monoclonal anti-human Akt,, rabbit monoclonal anti-human Phospho-EGF Receptor (p-EGFR; Tyr1068) and rabbit monoclonal anti-human Phospho-EGF Receptor were purchased from Cell Signaling Technology (Danvers, MA). Secondary HRP-linked goat anti-mouse or goat anti-rabbit IgG, were also purchased from Cell Signaling Technology (Danvers, MA).

Cells and clinical samples. For experiments on normal human counterpart Clonetics™ Astrocyte Cell System containing Normal Human Astrocytes (NHA) and an optimized medium for their growth was used (Lonza; Basel, Switzerland). Normal Human Astrocytes (NHA) are normal human cells derived from normal fetal human brain tissue and were cultured in recommended medium

Clonetics™ AGM™ BulletKit™ (Lonza; Basel, Switzerland). The human glioma cell lines U87MG (U87) were obtained from CLS Cell Lines Service GmbH (Eppelheim, Germany) or were kindly provided by Dr. Daniela Parolaro (University of Insubria, Italy). Small pieces of brain tissue containing tumor were collected at the time of craniotomy for tumor resection at the Neurosurgery Service of "G. Rummo" Medical Hospital (Benevento, Italy) and the Neurosurgery Service of "San Giovanni di Dio Ruggi d'Aragona" Medical Hospital (Salerno, Italy), divided into a portion immediately processed to generate primary tumor cell lines and a portion stored at –80°C for subsequent Western blot (WB) analysis. A second sample from each patient was also taken for clinical diagnosis performed by expert neuropathologists in accordance with the International Classification of CNS tumors drafted under the auspices of the World Health Organization (WHO). The tumors were diagnosed as astrocytoma (WHO grade I-III; n=3), glioma (WHO grade II, n=2) or glioblastoma multiforme (WHO grade IV; n=18). There were not significant differences by gender, or age between the different groups (Ciaglia et al., 2015). All tissue samples were collected in accordance with the ethical standards of the Institutional Committee. The patients had been informed about the establishment of cellular models from their tumors and had given informed consent in written form. The preparation of adherent primary cultures of brain tumor cells (designated as GBMn) was conducted as reported elsewhere. (Ciaglia et al., 2015)

Human glioma cell line U87MG was cultured in EMEM (Lonza) supplemented with 10% heat-inactivated fetal bovine serum (Euroclone), 1% L-glutamine, 1% antibiotic mixture, 1% sodium pyruvate, 1% non-essential aminoacids (Euroclone).

All cell cultures were maintained at 37°C in humidified 5 % CO2 atmosphere.

Determination of glioma cell proliferation. Glioma cells U87MG or normal human astrocytes (NHA) ($4x10^3$/well), were cultured for 24h into 96-well plates before addition of i6A at the indicated concentrations and cultured for additional 24, 48 and 72h at 37°C. Cell proliferation was evaluated by measuring BrdU incorporation into DNA (BrdU colorimetric assay kit; Roche Applied

Science, South San Francisco, CA, USA). Newly synthesized BrdU-DNA was determined on an ELISA plate reader (ThermoScientific) at 450 nm. All experiments were performed in triplicate, and the relative cell growth was expressed as a percentage comparison with the untreated control cells to control for unwanted source of variation.

Apoptosis analysis. Quantitative assessment of apoptosis of U87MG glioma cell line or normal human astrocytes (NHA) was analyzed by anti-human Annexin V (BioLegend, San Diego, CA, USA) and PI staining and processed as previously described (Malfitano et al., 2013). Briefly, cells grown in 100-mm dishes for 24, 48 and 72h in EMEM containing 2% FBS or in recommended medium AGM™ BulletKit™ (Lonza) were harvested with trypsin and washed in PBS. Following 24h of incubation, immunofluorescence staining was performed. The cells were resuspended in Annexin V binding buffer (10 mM HEPES/NaOH, pH 7; 140 mM NaCl; and 2.5 mM $CaCl_2$) and stained with Annexin V-FITC for 20 min at room temperature (RT) and then with PI at RT for additional 15 min in the dark. The cells were acquired by flow cytometer within 1 h after staining. At least 10,000 events were collected, and the data were analyzed by Cell- Quest Pro software (Becton Dickinson, San Jose, CA). Data are expressed as logarithmic values of fluorescence intensity.

Western blot (WB) analysis. For analysis of protein levels from cells they were grown in p60 tissue culture plates at a density of 2x104 cells/cm2 for 24 h. Tumor cells were then incubated with vehicle, i6A, CM223 or Zoledronic acid monohydrate in the presence or absence of EGF. After incubation cells were washed with PBS, harvested and lysed in ice-cold RIPA lysis buffer (50 mM Tris-HCl, 150 mM NaCl, 0.5% Triton X-100, 0.5% deoxycholic acid, 10 mg/ml leupeptin, 2 mM phenylmethylsulfonyl fluoride, and 10 mg/ml aprotinin). Tumor pieces were disrupted for protein extraction by gentle homogenization (Potter-Elvehjem Pestle) in cold RIPA buffer. After removal of cell debris by centrifugation (14,500 g for 20 min at 4°C), the proteins were estimated. About

30µg of proteins was loaded on 10, 12 or 15% SDS–polyacrylamide gels under reducing conditions and then transferred to nitrocellulose membranes. The blots were blocked with 5% nonfat dry milk (Bio-Rad, Richmond, CA, USA) in Tris-buffered saline containing 0.1% Tween-20 (TBST) for 1 h at room temperature and incubated with the specific antibody. Immunodetection of specific proteins was carried out with horseradish peroxidase-conjugated donkey anti-mouse or anti-rabbit IgG (Biorad, Hercules, CA), using the enhanced chemiluminescence (ECL) system (Amersham Pharmacia Biotech, Piscataway, NJ) according to the manufacturer's instructions and then exposed to X-ray film (Amersham Biosciences). Immunoreactive bands were quantified with Quantity One 1-D analysis software (Bio-Rad). To ascertain equal protein loading in Western blots of cell lysates, membranes were probed with an antibody raised to α-tubulin (Sigma-Aldrich, St. Louis, MO, USA) or β-actin (Abcam, Cambridge, UK).

siRNA-Mediated Knockdown

FPPS siRNA transfection was carried out according to manufacturer's instructions. First, siRNA FPPS (Ambion) and negative control siRNA (Silencer Negative Control, Ambion) were dissolved in Opti-MEM serum-free media. Both FPPS and scrambled siRNA were delivered into the U87 cell cultures plated 18 hours before transfection (approximately 80% confluency) via Lipofectamine 3000 (#L3000-001, Invitrogen). The final concentration of FPPS and scrambled siRNA in culture was 100nM. The cells were incubated with the transfection reagents for 48 hours. Then, cell media was replaced with serum-free media to induce starvation and treated with 10 µM CM223 for 8 hours. After that EGF was added (final concentration 50ng/mL) for 10 minutes. The cells were then harvested for analysis of protein knockdown via western blot and tested for cell signaling experiments.

FPPS gene expression. The plasmid p11, transformed into BL21(DE3)-pLysS cells, was purchased from SGC-Oxford and contained the T7/Lac promoter and ampicillin resistance. FPPS

was expressed in *Escherichia coli* as a fusion protein (67−419 residues) with a N-terminal poly-histidine tail and a mutation (threonin with serine) on residue 266, molecular weight 43kDa. For expression in *E. coli*, bacterial clones were grown in 1L of LB (Luria-Bertani) medium containing 50μg/mL ampicillin. Cell growth was monitored spectrophotometrically by measuring OD_{600} nm periodically. When growth was performed to an OD_{600} of 0.7 at 37°C, the 1mM isopropyl-D-thiogalactoside (IPTG) was added. IPTG was purchased from Sigma- Aldrich (St. Louis, MO). After 6h of cell growth, cells were pelleted by centrifugation and re-suspended in lysis buffer (50 mL of 5% glycerol, 5 mM imidazole, 500 mM NaCl, 50 mM PBS (pH 7.5)) and sonicated. Protein was purified with His-Trap HP column at 1 mL/min using an AKTA purifier system, the soluble extract was applied to a nickel-chelated agarose affinity column that had been equilibrated with the same buffer. The protein was eluted from the column with elution buffer (5% glycerol, 250 mM imidazole, 500 mM NaCl, 50 mM PBS (pH 7.5)). Affinity chromatography on a nickel chelated agarose column permitted a simple one step protein purification. Therefore FPPS was transferred into Vivaspin 20 concentrator, cutoff 3kDa, to exchange the buffer for NMR studies.

NMR Sample Preparation. All chemicals were purchased from Sigma-Aldrich (St. Louis, MO). i6A was purchased from Iris Biotech GMBH and zoledronic acid from Sigma-Aldrich (St. Louis, MO). i6A analogs were synthesize at University of Pisa and University of Milano. STD-NMR and WaterLOGSY experiments were recorded at 25°C on Bruker AV600 MHz spectrometer at a ^{1}H resonance frequency of 600 MHz equipped with a 5 mm triple resonance $^{1}H(^{13}C/^{15}N)$, z-axis pulsed-field gradient probe head. For characterization purposes, i6A samples consisted of a 5mM solution in 25 mM d-Tris, pH 7.4, 0.5 mM $MgCl_2$, and 25 mM NaCl with 1% dimethyl sulfoxide-d6 as a co-solvent, and the spectra were referenced to residual solvent. $^{1}H-^{1}D$ spectra were acquired at a resolution of 16k complex points in the time domain with 32 accumulations each (sw=6000 Hz, d1=3s). The FPPS protein at 8 μM concentration was titrated with i6A-analogs to have protein/ligands molar ratios 1:10, 1:20, 1:30, 1:50, 1:70, and 1:100. For each addition of ligands,

STD build-up experiment was carried out using different saturation times (0.50, 1.00, 1.50, 2.00, 3.00, 4.00, and 5.00s and different relaxation delay 1.50, 2.00, 2.50, 3.00, 4.00, 5.00, and 6.00s). For each experiment in the frequency list (FQ2LIST), the on-resonance and off-resonance pulse were 320 and 50000 Hz, respectively. Briefly, two free induction decay (FID) data sets were collected in an interleaved manner to minimize temporal fluctuations with the protein irradiation frequency set on-resonance (−0.5 ppm) and off-resonance (40 ppm), respectively (sw = 6000 Hz, 16 steady state scans, 2048 transients, 4k complex points, d1 = 3s). Protein saturation was obtained using a train of individual 50 ms long, frequency selective Gaussian radio frequency (rf) pulses separated by an inter pulse delay of 1ms. The FID acquired with off-resonance irradiation generated the reference spectrum (I_{off}), whereas the difference FID (off-resonance on-resonance) yielded the STD spectrum (ISTD = I_{off} - I_{on}). Spectra were processed with an exponential apodization function (^{1}Hz line broadening) and zero-filling to 8k complex points before Fourier transformation and baseline correction with a third order Bernstein polynomial fit. The STD measurements were done in duplicate, and all data were processed and analyzed using TopSpin software (Bruker v 1.3).

FPPS colorimetric assay. The colorimetric assays were performed in 96-well plates, flat bottom. 200 ng of fresh pure FPPS was assayed in a final volume of 100 µl buffer (50mM Tris pH 7.5, 2mM MgCl2, 1mM DTT, 5 µg/ml BSA) with or without pre-incubation with inhibitors (i6A 1-10mM, **CM223** 0.1-5.0mM, zoledronic acid 1-2 µM as positive control) for 30 min. at 37 °C. The reaction was initiated by the addition of the substrates dimetilallil pirophosphate (DMAPP 50 µM and IPP 50 µM) and proceeded for 1 hour at 37 °C. 10 µl of 2.5% ammonium molybdate reagent (in 5 N H_2SO_4) were added and incubated for 10 min to allow the formation of PPi-molybdate complex, finally the complex was reduced by 10 µl of 0.5 M 2 -mercaptoethanol and 5 µl of Eikonogen reagent (0.25 g of sodium sulfite and 14.7 g of meta-bisulfite were dissolved in 100 ml water). Plates were incubated with gentle mixing on a plate shaker for 20 min. The absorbance was measured at 580 nm employing a microplate reader. The control experiments were carried out with

incubation mixture in the absence of substrate or FPPS for background deduction. To set the conditions, a standard curve using $Na_2P_2O_7$ as the source of PPi (Fig. S6) was constructed.

Docking Studies. AutoDock version 4.2(Morris et al., 2009) and AutoDock Vina version 1.0(Trott & Olson, 2010) in combination with the LGA were used for all docking calculations. The starting conformations for docking studies of **CM223** and **FP13** ligands were built with Maestro (version 9.6). (Schrödinger, 2009) Three-dimensional starting model of each compounds for the subsequent docking calculations, were preliminary optimized by conjugate gradient, (0.05Å convergence threshold).

3D FPPS protein model was obtained from Protein Data Bank database (PDB code: 1ZW5). (Kavanagh et al., 2006) Water molecules were removed, and the obtained file was then processed with Autodock Tools 1.5.6, merging non-polar hydrogens and adding Gasteiger charges.

For both docked ligands, all bonds were considered rotable. For an exhaustive exploration of conformational space, 6 docking calculations consisting of 250 runs were performed, yielding 1500 structures. An initial population of 450 randomly placed individuals, a maximum number of $5x10^6$ energy evaluations, and a maximum number of $4x10^6$ generations were taken into account. The mutation and crossover rates used were 0.02 and 0.80, respectively. The local search probability was 0.26. For all docking calculations, a grid box size of 53 65 57 points (spacing between the grids points of 0.375Å) was used, centered on the center of the target binding site.

The resulting data, differing by less than 3.5 Å in positional rmsd, were clustered together and represented by the result with the most favorable free energy of binding. All 3D models were depicted using Python and VMD. (Humphrey, Dalke & Schulten, 1996).

Nomenclature of Targets and Ligands. Key protein targets and ligands in this article are hyperlinked to corresponding entries in http://www.guidetopharmacology.org, the common portal for data from the IUPHAR/BPS Guide to PHARMACOLOGY (Southan et al., 2016), and are

permanently archived in the Concise Guide to PHARMACOLOGY 2015/16 (Alexander et al., 2015).

Statistical analysis. Statistical analysis was performed in all the experiments shown by using the GraphPad prism 6.0software for Windows (GraphPad software). For each type of assay or phenotypic analysis, data obtained from multiple experiments are calculated as mean ± SD and analyzed for statistical significance using the 2- tailed Student t-test, for independent groups, or ANOVA followed by Tukey's post-hoc test for multiple comparisons, when F achieved was $P<0.05$ and there was no significant variance inhomogeneity. Minimal statistical significance was set at $*P<0.05$. Some results were normalized to control for unwanted source of variation. To ensure reproducibility of the results and minimize bias, the use of authenticated U87MG and NHA at the same passage and wherever possible, the same manufactures' kit and reagents were used for selected experiments. For the control of bias, all data generated during study have been recorded directly, promptly, accurately, and legibly by a dedicated individual entering the data. The data and statistical analysis comply with the recommendations on experimental design and analysis in pharmacology (Curtis et al., 2015)

▪ AUTHOR INFORMATION

Corresponding Authors

*For M.B.: phone, +39-089-965217; fax, +39-089-969602; Email, maubiful@unisa.it.

*For A.M.D.: phone, +39-089-969748; fax, +39-089-969602; Email, dursi@unisa.it.

- **ACKNOWLEDGMENTS**
- This study was supported by Associazione Italiana Ricerca sul Cancro (AIRC; IG 18999 and IG13312 to M. Bifulco,). E. Ciaglia was supported by a fellowship from Fondazione Umberto Veronesi (FUV 2017, cod.1072).. The authors thank Dr. Francesco Montella and Dr. Ylenia Senatore (University of Salerno) for their continual support.

ABBREVIATIONS USED

i6A, N6-isopentenyladenosine; FPPS, farnesyl pyrophosphate synthase; CCR2, chemokine receptor 2; CCL2, chemokine ligand 2; CCR5, CC chemokine receptor 5; COSY, correlated spectroscopy; DMAPP, dimetilallil pirofosfato FEP, free energy perturbation; IPP, isopentenyl pyrophosphate; TI, thermodynamic integration; LIE, linear interaction energy; NK, natural killer; N-BP, nitrogen-containing bisphosphonates; NMR, nuclear magnetic resonance; PBS, phosphate buffered saline; PI, propidium iodide; STD, saturation transfer difference; TLC, thin layer chromatography; tRNA, tRNA.

Authors contributions: E.C. wrote the paper, designed and conducted biological assays and analyzed and interpreted data; M.G. conducted FPPS gene expression procedure, NMR studies and analyzed and interpreted data; M.A. performed biological research, analyzed data and reviewed critically the paper; M.S. performed Molecular Docking studies; C.L. performed research, R.R., S.P. and P.G. performed siRNA transfection procedure and established primary derived cells. M.R., C.M. and P.C. conducted the synthesis of new i6A derivatives and gave substantial contribution to analysis and interpretation of data; A.M.D. and M.B. supervised the project in its entirety, wrote and reviewed critically the paper and provided financial support. All authors approved the final version to be published.

REFERENCES

Alexander SP, Kelly E, Marrion N, Peters JA, Benson HE, Faccenda E, *et al.* (2015). The Concise Guide to PHARMACOLOGY 2015/16: Overview. Br J Pharmacol. 172(24):5729-43.

Angulo J, & Nieto PM (2011). STD-NMR: application to transient interactions between biomolecules-a quantitative approach. Eur Biophys J 40**:** 1357-1369.

Bifulco M, Malfitano AM, Proto MC, Santoro A, Caruso MG, & Laezza C (2008). Biological and pharmacological roles of N-6-Isopentenyladenosine: An emerging anticancer drug. Anticancer Agents Med Chem 8**:** 200-204.

Carlberg M, Dricu A, Blegen H, Wang M, Hjertman M, Zickert P, *et al.* (1996). Mevalonic acid is limiting for N-linked glycosylation and translocation of the insulin-like growth factor-1 receptor to the cell surface. Evidence for a new link between 3-hydroxy-3-methylglutaryl-coenzyme a reductase and cell growth. J Biol Chem 271**:** 17453-17462.

Castiglioni S, Casati S, Ottria R, Ciuffreda P, & Maier JAM (2013). N6-Isopentenyladenosine and its Analogue N6-Benzyladenosine Induce Cell Cycle Arrest and Apoptosis in Bladder Carcinoma T24 Cells. Anticancer Agents Med Chem 13**:** 672-678.

Ceresa BP, & Bahr SJ (2006). rab7 activity affects epidermal growth factor:epidermal growth factor receptor degradation by regulating endocytic trafficking from the late endosome. J Biol Chem 281**:** 1099-1106.

Chen YZ, & Zhi DG (2001). Ligand-protein inverse docking and its potential use in the computer search of protein targets of a small molecule. Proteins-Structure Function and Genetics 43**:** 217-226.

Ciaglia E, Abate M, Laezza C, Pisanti S, Vitale M, Seneca V, *et al.* (2017). Antiglioma effects of N6-isopentenyladenosine, an endogenous isoprenoid end product, through the Downregulation of Epidermal Growth Factor Receptor. Int J Cancer 140:959-972.

Ciaglia E, Pisanti S, Picardi P, Laezza C, Malfitano AM, D'Alessandro A, *et al.* (2013). N6-isopentenyladenosine, an endogenous isoprenoid end product, directly affects cytotoxic and regulatory functions of human NK cells through FDPS modulation. J Leukocyte Biol 94**:** 1207-1219.

Ciaglia E, Torelli G, Pisanti S, Picardi P, D'Alessandro A, Laezza C, *et al.* (2015). Cannabinoid receptor CB1 regulates STAT3 activity and its expression dictates the responsiveness to SR141716 treatment in human glioma patients' cells. Oncotarget 6**:** 15464-15481.

- Curtis MJ, Bond RA, Spina D, Ahluwalia A, Alexander SP, Giembycz MA *et al.* (2015), Experimental design and analysis and their reporting: new guidance for publication in BJP. Br J Pharmacol 172:3461-71.

Fournier PGJ, Dauhine F, Lundy MW, Rogers MJ, Ebetino FH, & Clezardin P (2008). Lowering Bone Mineral Affinity of Bisphosphonates as a Therapeutic Strategy to Optimize Skeletal Tumor Growth Inhibition In vivo. Cancer Res 68**:** 8945-8953.

Frische EW, & Zwartkruis FJT (2010). Rap1, a mercenary among the Ras-like GTPases. Dev Biol 340**:** 1-9.

Furnari FB, Cloughesy TF, Cavenee WK, & Mischel PS (2015). Heterogeneity of epidermal growth factor receptor signalling networks in glioblastoma. Nat Rev Cancer 15**:** 302-310.

Gao JB, Chu XS, Qiu YG, Wu L, Qiao YQ, Wu JS, *et al.* (2010). Discovery of potent inhibitor for farnesyl pyrophosphate synthase in the mevalonate pathway. Chem Commun 46**:** 5340-5342.

Gibbs JB, Oliff A, & Kohl NE (1994). Farnesyltransferase inhibitors: Ras research yields a potential cancer therapeutic. Cell 77**:** 175-178.

Gordon S, Helfrich MH, Sati HIA, Greaves M, Ralston SH, Culligan DJ, *et al.* (2002). Pamidronate causes apoptosis of plasma cells in vivo in patients with multiple myeloma. Br J Haematol 119**:** 475-483.

Hackel PO, Zwick E, Prenzel N, & Ullrich A (1999). Epidermal growth factor receptors: critical mediators of multiple receptor pathways. Curr Opin Cell Biol 11**:** 184-189.

Hamdi M, Popeijus HE, Carlotti F, Janssen JM, van der Burgt C, Cornelissen-Steijger P, *et al.* (2008). ATF3 and Fra1 have opposite functions in JNK-and ERK-dependent DNA damage responses. DNA Repair 7**:** 487-496.

Hocek M, Holy A, Votruba I, & Dvorakova H (2000). Synthesis and cytostatic activity of substituted 6-phenylpurine bases and nucleosides: Application of the Suzuki-Miyaura cross-coupling reactions of 6-chloropurine derivatives with phenylboronic acids. J Med Chem 43**:** 1817-1825.

Humphrey W, Dalke A, & Schulten K (1996). VMD: visual molecular dynamics. J Mol Graphics 14**:** 33-38.

Jahnke W, Rondeau JM, Cotesta S, Marzinzik A, Pelle X, Geiser M, *et al.* (2010). Allosteric non-bisphosphonate FPPS inhibitors identified by fragment-based discovery. Nat Chem Biol 6**:** 660-666.

Jeyaraj SC, Unger NT, & Chotani MA (2011). Rap1 GTPases: an emerging role in the cardiovasculature. Life Sci 88**:** 645-652.

Kavanagh KL, Guo K, Dunford JE, Wu X, Knapp S, Ebetino FH, *et al.* (2006). The molecular mechanism of nitrogen-containing bisphosphonates as antiosteoporosis drugs. Proc Natl Acad Sci U S A 103**:** 7829-7834.

Kersten H (1984). On the biological significance of modified nucleosides in tRNA. Prog Nucleic Acid Res Mol Biol 31**:** 59-114.

Laezza C, Caruso MG, Gentile T, Notarnicola M, Malfitano AM, Di Matola T, *et al.* (2009). N6-isopentenyladenosine inhibits cell proliferation and induces apoptosis in a human colon cancer cell line DLD1. Int J Cancer 124**:** 1322-1329.

Laezza C, Caruso MG, Gentile T, Notarnicola M, Malfitano AM, Di Matola T, *et al.* (2014). N6-isopentenyladenosine inhibits cell proliferation and induces apoptosis in a human colon cancer cell line DLD1 (vol 124, pg 1322, 2009). Int J Cancer 135**:** E11-E11.

Laezza C, D'Alessandro A, Di Croce L, Picardi P, Ciaglia E, Pisanti S, *et al.* (2015). p53 regulates the mevalonate pathway in human glioblastoma multiforme. Cell Death Dis 6.

Laezza C, Malfitano AM, Di Matola T, Ricchi P, & Bifulco M (2010). Involvement of Akt/NF-kappaB pathway in N6-isopentenyladenosine-induced apoptosis in human breast cancer cells. Mol Carcinog 49**:** 892-901.

Laezza C, Notarnicola M, Caruso MG, Messa C, Macchia M, Bertini S, *et al.* (2006). N6-isopentenyladenosine arrests tumor cell proliferation by inhibiting farnesyl diphosphate synthase and protein prenylation. Faseb J 20**:** 412-418.

Laten HM, & Zahareasdoktor S (1985). Presence and Source of Free Isopentenyladenosine in Yeasts. Proc Natl Acad Sci U S A 82**:** 1113-1115.

Lauro G, Romano A, Riccio R, & Bifulco G (2011). Inverse Virtual Screening of Antitumor Targets: Pilot Study on a Small Database of Natural Bioactive Compounds. J Nat Prod 74**:** 1401-1407.

Malfitano AM, Laezza C, Saccomanni G, Tuccinardi T, Manera C, Martinelli A, *et al.* (2013) Immune-modulation and properties of absorption and blood brain barrier permeability of 1,8-naphthyridine derivatives. J Neuroimmune Pharmacol. 8(5):1077-86.

Mayer M, & Meyer B (1999). Characterization of ligand binding by saturation transfer difference NMR spectroscopy. Angew Chem Int Ed 38**:** 1784-1788.

Mayer M, & Meyer B (2001). Group epitope mapping by saturation transfer difference NMR to identify segments of a ligand in direct contact with a protein receptor. J Am Chem Soc 123**:** 6108-6117.

Morris GM, Huey R, Lindstrom W, Sanner MF, Belew RK, Goodsell DS, *et al.* (2009). AutoDock4 and AutoDockTools4: Automated docking with selective receptor flexibility. J Comput Chem 30**:** 2785-2791.

Ottria R, Casati S, Baldoli E, Maier JA, & Ciuffreda P (2010). N(6)-Alkyladenosines: Synthesis and evaluation of in vitro anticancer activity. Bioorg Med Chem 18**:** 8396-8402.

Pisanti S, Picardi P, Ciaglia E, Margarucci L, Ronca R, Giacomini A, *et al.* (2014). Antiangiogenic effects of N6-isopentenyladenosine, an endogenous isoprenoid end product, mediated by AMPK activation. Faseb J 28**:** 1132-1144.

Sacchettini JC, & Poulter CD (1997). Biochemistry - Creating isoprenoid diversity. Science 277**:** 1788-1789.

Schrödinger M (2009). LLC New YorkNY.

Scrima M, Lauro G, Grimaldi M, Di Marino S, Tosco A, Picardi P, *et al.* (2014). Structural Evidence of N6-Isopentenyladenosine As a New Ligand of Farnesyl Pyrophosphate Synthase. J Med Chem 57**:** 7798-7803.

Sigismund S, Algisi V, Nappo G, Conte A, Pascolutti R, Cuomo A, *et al.* (2013). Threshold-controlled ubiquitination of the EGFR directs receptor fate. The EMBO Journal 32:2140–2157.

Southan C, Sharman JL, Benson HE, Faccenda E, Pawson AJ, Alexander SP *et al.* (2016). The IUPHAR/BPS Guide to PHARMACOLOGY in 2016: towards curated quantitative interactions between 1300 protein targets and 6000 ligands. Nucl Acids Res 44: D1054-1068.

Spinola M, Colombo F, Falvella FS, & Dragani TA (2007). N6-isopentenyladenosine: a potential therapeutic agent for a variety of epithelial cancers. Int J Cancer 120**:** 2744-2748.

Szkopinska A, & Plochocka D (2005). Farnesyl diphosphate synthase; regulation of product specificity. Acta Biochim Pol 52**:** 45-55.

Thurnher M, Nussbaumer O, & Gruenbacher G (2012). Novel Aspects of Mevalonate Pathway Inhibitors as Antitumor Agents. Clin Cancer Res 18**:** 3524-3531.

Trott O, & Olson AJ (2010). AutoDock Vina: improving the speed and accuracy of docking with a new scoring function, efficient optimization, and multithreading. J Comput Chem 31**:** 455-461.

Villa GR, Hulce JJ, Zanca C, Bi J, Ikegami S, Cahill GL, *et al.* (2016). An LXR-Cholesterol Axis Creates a Metabolic Co-Dependency for Brain Cancers. Cancer Cell 30**:** 683-693.

Wang J-C, Chu P-Y, Chen C-M, & Lin J-H (2012). idTarget: a web server for identifying protein targets of small chemical molecules with robust scoring functions and a divide-and-conquer docking approach. Nucleic Acids Res 40**:** W393-W399.

Wang Y, Panasiuk A, & Grainger DW (2011). Small interfering RNA knocks down the molecular target of alendronate, farnesyl pyrophosphate synthase, in osteoclast and osteoblast cultures. Mol Pharm 8**:** 1016-1024.

Warren CM, & Landgraf R (2006). Signaling through ERBB receptors: multiple layers of diversity and control. Cell Signal 18**:** 923-933.

Wei F, Yan J, & Tang D (2011). Extracellular signal-regulated kinases modulate DNA damage response - a contributing factor to using MEK inhibitors in cancer therapy. Curr Med Chem 18**:** 5476-5482.

Woo IS, Eun SY, Kim HJ, Kang ES, Kim HJ, Lee JH, *et al.* (2010). Farnesyl diphosphate synthase attenuates paclitaxel-induced apoptotic cell death in human glioblastoma U87MG cells. Neurosci Lett 474**:** 115-120.

Figure Legends

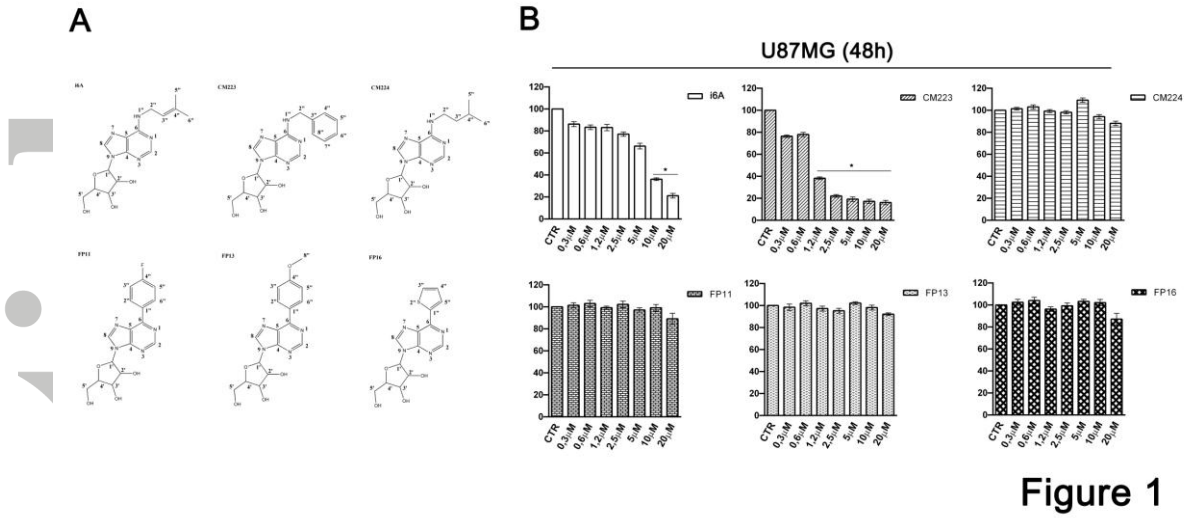

Figure 1. Effect of i6A and analogs on cellular proliferation of human glioma cell line (U87MG). ***A*** i6A analogs structures: chemical structure of FP11, FP13, FP16, CM223, CM224 and of i6A for comparison. ***B*** U87MG cells were cultured for 48 h in the presence of the indicated concentrations (0-20 µM) of i6A, CM223, CM224, FP11, FP13 or FP16 before analysis of cell proliferation by BrdU incorporation assay. Results are expressed as means ± SD of 5 independent experiments performed in triplicate and reported as percentage *vs* the untreated control (ANOVA, *P<0.05 *vs* control).

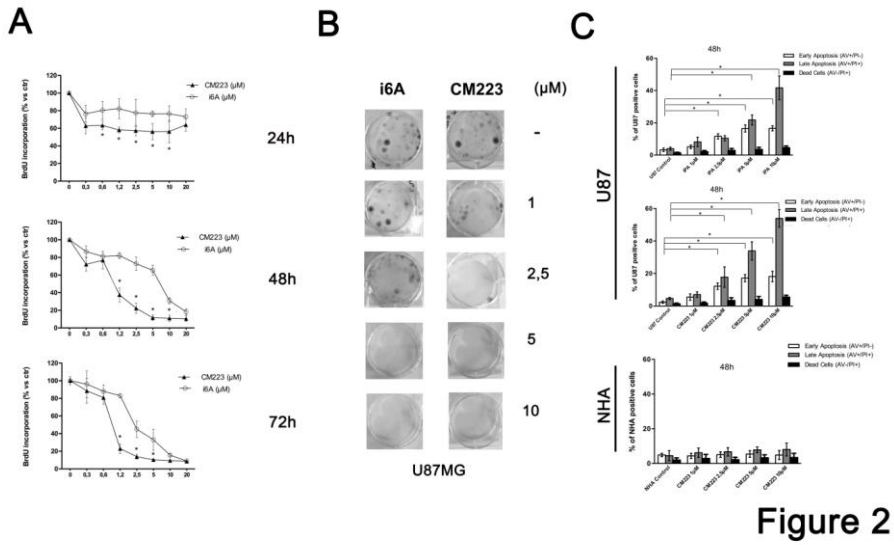

Figure 2

Figure 2. Comparison of the effect of i6A and CM223 on cellular integrity of human glioma cell line (U87MG) and normal human astrocytes (NHA). ***A*** U87MG cells were cultured for 24, 48 and 72 h in the presence of the indicated concentrations (0-20 μM) of i6A or CM223 before analysis of cell proliferation by BrdU incorporation assay. Results are expressed as means ± SD of 5 independent experiments performed in triplicate and reported as percentage *vs* the untreated control (ANOVA, *P<0.05 *vs* control) ***B*** Representative images of the clonogenic assay on glioma cell line U87MG, 10 days after treatment with i6A and CM223 at the indicated concentrations (0-10 μM). The experiment was conducted two times in triplicate. ***C*** Induction of apoptosis measured by Annexin V and propidium iodide (PI) double staining through flow cytometry in i6A or CM223-treated U87MG cells (*upper panels*) and in CM223-treated NHA (*lower panel*) after 48h. Histograms indicate total percentage of early (Annexin V-positive cells/ PI-negative cells) and late apoptotic events (Annexin V/ PI-double positive cells) as well as necrotic cells (Annexin V-negative cells/ PI-positive cells). Results are representative of 5 independent experiments performed in duplicate and expressed as mean ± SD (ANOVA, *P<0.05 *vs* untreated control cells).

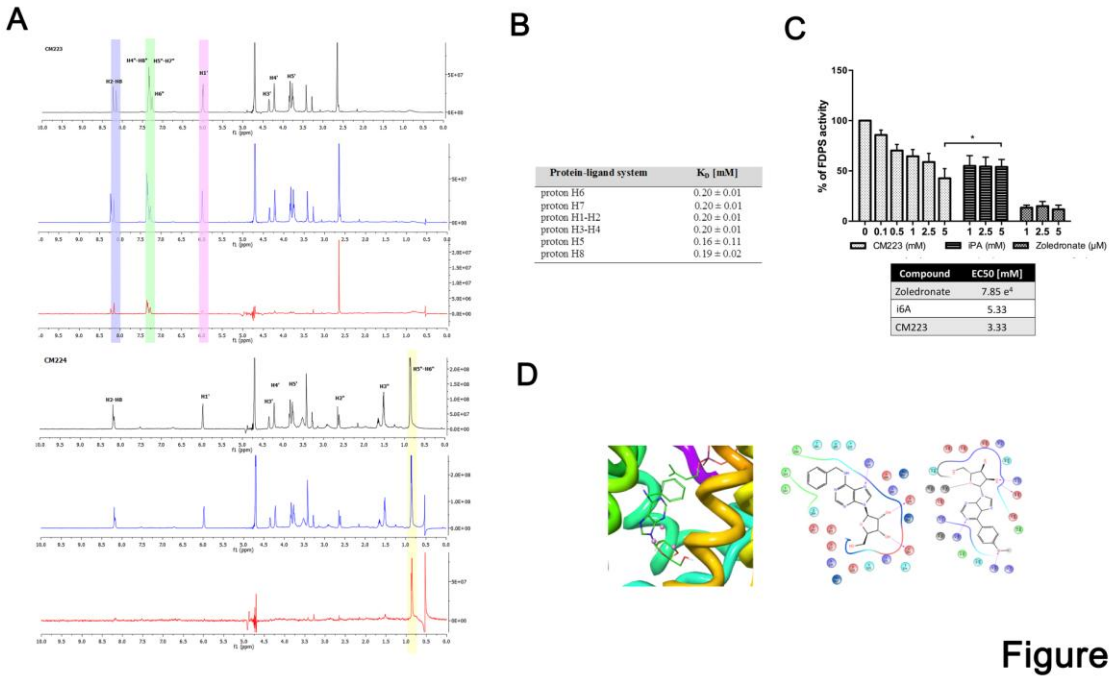

Figure 3

Figure 3. Evaluation of the biological significance of the FPPS-CM223 interaction in U87MG glioma cells. ***A*** STD-NMR spectra of FPPS-CM223 (*left*) and FPPS-CM224 (*right*), in black the off-resonance spectra, in blue the on-resonance spectra and in red the STD spectra. ***B*** Dissociation constants of the FPPS-CM223 complex ***C*** FPPS activity after the pre-treatment with CM223 (from 0.1 to 5 mM, 30 min 37 °C) and i6A (from 1 to 5 mM, 30 min 37 °C). The potent FPPS inhibitor, zoledronic acid (1-2 μM, 30 min 37 °C) was used as positive control. The inhibitory activity of CM223 with respect to i6A was evaluated. Results are expressed as mean ± SD of n=5 experiments. (ANOVA, *P<0.05 versus i6A). ***D*** *Left:* Molecular docking prediction of CM223 ligand in the FPPS binding site (CM223 colored by atom type: C green, O red, H white, N blue, Mg2+ pink). FPPS backbone was represented as ribbon. *Centre and Right*: 2D interactions panel showing peculiar interaction of CM223 and FPPS residues (*centre*) and 2D interactions panel showing peculiar interaction of FP13 and FPPS residues (*right*) (Red: charged negative, Violet: charged positive, Cyano: polar, Green: Hydrophobic, Blue: Mg2+).

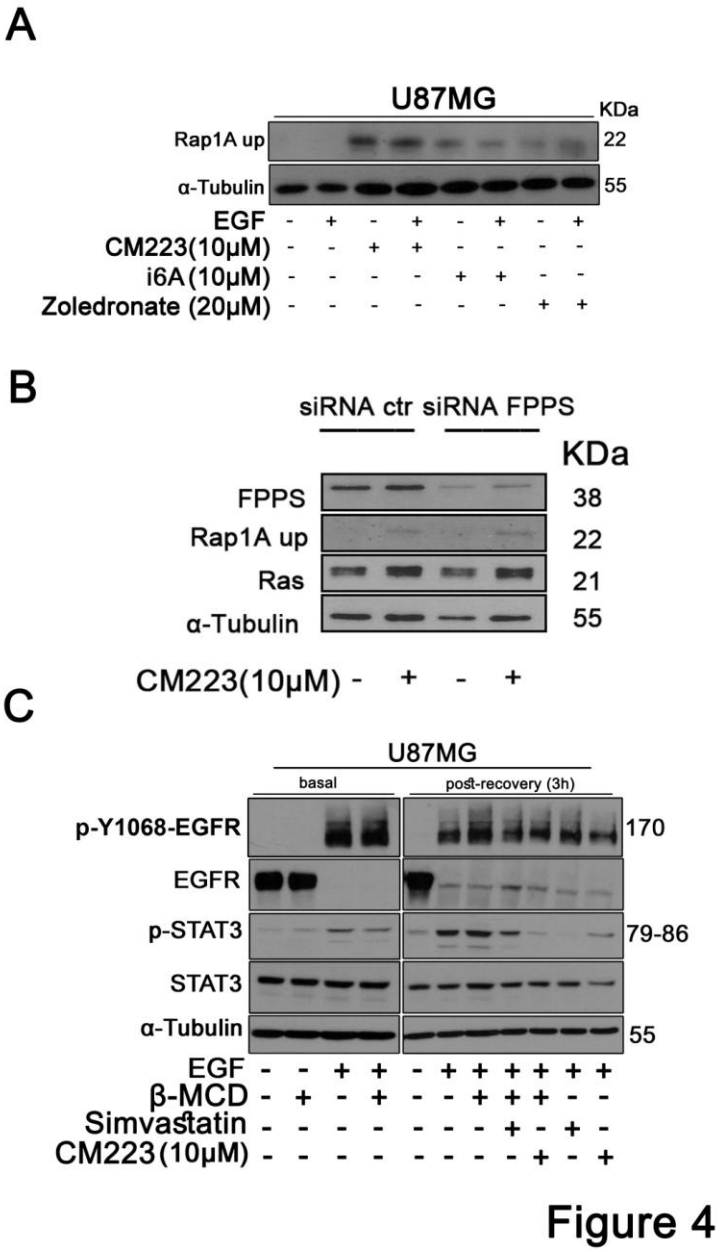

Figure 4

Figure 4. Analysis of CM223-induced block of isoprenylation and its effects on EGFR status. ***A*** Western blot analysis of Rap1A-up on whole cell extracts from cell line U87MG cultured for 24h in the presence of the indicated concentrations (10 μM) of CM223, i6A(10 μM) or Zoledronate (20 μM), in the presence or absence of EGF (50ng/ml); α-tubulin was used as control of protein loading. Panel shows a representative Western blot of 3 different experiments performed with similar results. ***B*** Western Blot analysis of Rap1A-up and Ras in siCTR- and siFPPS transfected U87MG cells cultured alone or in the presence of the indicated concentrations (10 μM) of CM223 for 8h; α-tubulin was used as control of protein loading. Panel shows a representative Western blot of 3 different experiments performed with similar results. ***C*** Western blot analysis for p-Y1068 EGFR, total EGFR, p-STAT3 and total STAT3 on whole cell extracts from U87MG cells stimulated for 10 min with EGF (50ng/ml). U87MG cells were serum starved for 18h and then

incubated with and without methyl-β-cyclodextrins (10 mM) for 15 min at 37°C. After that, in basal condition (*left panel*) U87MG cells were stimulated for 10 min with EGF (50ng/ml) or alternatively (*right panel*) the cells were left to recover signaling in serum free control medium in presence or absence of CM223 and/or Simvastatin (20 μM) for 3h and then stimulated with EGF for 10 min. α-tubulin was used as control of protein loading. The panel shows a representative Western blot of 2 different experiments performed with similar results**.**

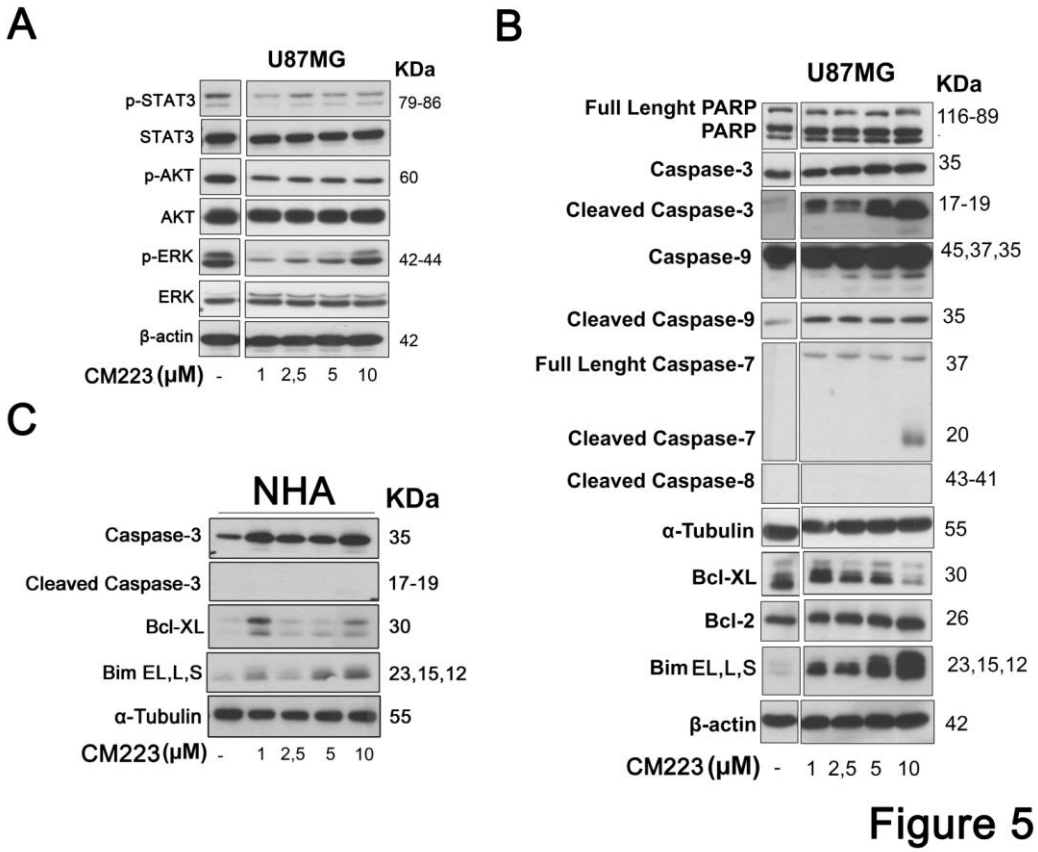

Figure 5. CM223-mediated modulation of oncogenic signaling pathways and proteins of the apoptotic process in U87 and NHA. ***A*** Western blot analysis for p-STAT3, total STAT3, p-AKT, total AKT, p-ERK and total ERK on whole cell extracts from cell line U87MG cultured for 24h in the presence of the indicated concentrations (0-20 μM) of CM223; β-actin was used as control of protein loading. Panel shows a representative Western blot of 3 different experiments performed with similar results. ***B*** Western blot analysis for PARP, Caspase-3, Cleaved Caspase-3, Caspase-9, Cleaved Caspase-9, Full Length and Cleaved Caspase-7, Cleaved Caspase-8, Bcl-XL, Bcl-2 and Bim, on whole cell extracts from cell line U87MG cultured for 24h in the presence of the indicated concentrations (0-20 μM) of CM223. β-actin and α-tubulin were used as control of protein loading. Panel shows a representative Western blot of 3 different experiments performed with similar results. ***C*** Western blot analysis for Caspase-3, Cleaved Caspase-3, Bcl-XL and Bim on whole cell extracts from cell line NHA cultured for 24h in the presence of the indicated concentrations (0-20 μM) of CM223; α-tubulin was used as control of protein loading. Panel shows a representative Western blot of 3 different experiments performed with similar results.

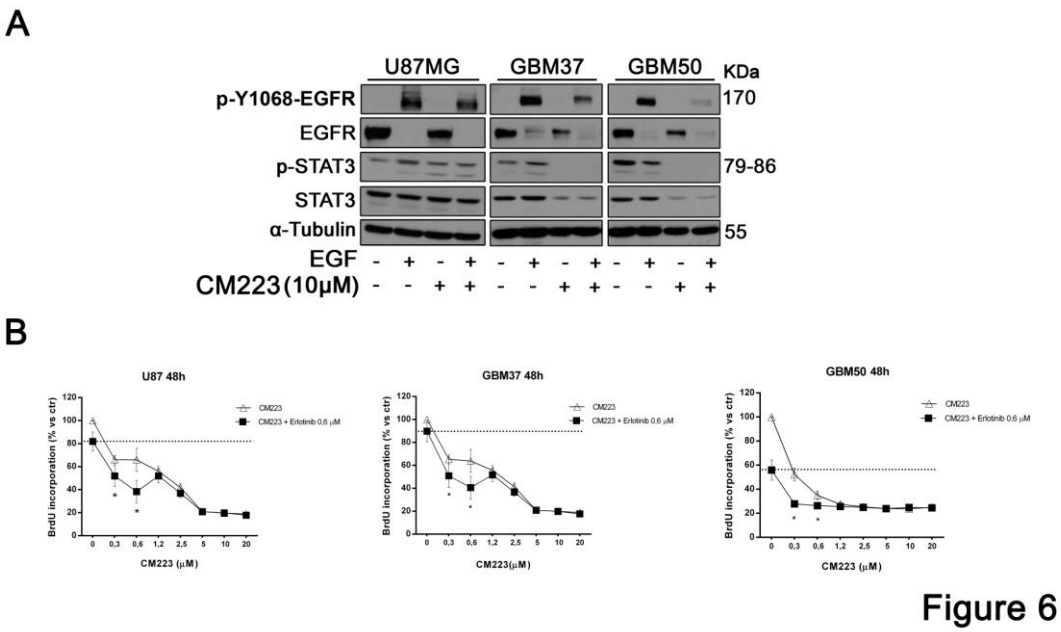

Figure 6. CM223 inhibits EGF/EGFR signaling in glioma patients derived-cells. ***A*** Western blot analysis for p-Y1068-EGFR, EGFR, p-STAT3 and total STAT3 in whole cell extracts from selected patients-derived primary cell lines (GBM37 and GBM50) serum starved and cultured for 18h with CM22310 μM and then stimulated or not with EGF (50ng/ml) for 10 minutes. α-tubulin was used as control of protein loading. Panels show representative Western blots of 2 different experiments performed with similar results. B U87MG cells and 2 representative patients-derived primary cell lines (GBM37 and GBM50) were treated for 48h with erlotinib (0.6 μM) in the presence or absence of the indicated concentrations (0-20 μM) of CM223 before analysis of cell proliferation by BrdU incorporation assay. Results, reported as percentage, are expressed as mean ± SD of 6 independent experiments performed in triplicate. (ANOVA, *P<0.05 vs untreated control cells).

Table of Links

TARGETS

EGFR: **epidermal growth factor receptor**
AKT: AKT serine/threonine kinase 1
ERK: mitogen-activated protein kinase 1
Rap: **RAS subfamily**
FPPS: (FPPS)

LIGANDS

FPP: **trans,trans-farnesyl diphosphate**
Erlotinib: Erlotinib

The isoprenoid derivative N6-benzyladenosine (CM223) exerts antitumor effect in glioma patient-derived primary cells through the mevalonate pathway.

Elena Ciaglia,[a] Manuela Grimaldi,[b] Mario Abate,[a] Mario Scrima,[b] Manuela Rodriquez,[b] Chiara Laezza,[c] Roberta Ranieri,[a] Simona Pisanti,[a] Pierangela Ciuffreda,[d] Clementina Manera,[e] Patrizia Gazzerro,[b] Anna Maria D'Ursi*[b] and Maurizio Bifulco*[a,f].

Substitution of isopentenyl with benzyl ring in N6-isopentenyl adenosine results in compound **CM223** capable of binding and inhibiting FPPS enzyme. It may be considered a new lead compound for the design of new FPPS inhibitors.